
# High field conduction in mineral oil based zno nanofluids prior to negative streamer inception

# High field conduction in mineral oil based ZnO nanofluids prior to negative streamer inception

Journal of Physics Communications

PAPER

# High field conduction in mineral oil based ZnO nanofluids prior to negative streamer inception

Marley Becerra[1], Mauricio Aljure[1,2], Amir Masoud Pourrahimi[3,4] and Francisco Roman[5]

[1] School of Electrical Engineering and Computer Science, KTH Royal Institute of Technology, SE-100 44 Stockholm, Sweden
[2] BioGRID Grupo de Investigación y Desarrollo en Ciencias, Tecnología e Innovación, SoPhiC Sociedad de Doctores e Investigadores de Colombia, Bogotá, Colombia
[3] Department of Chemistry and Chemical Engineering, Chalmers University of Technology, SE-412 96, Gothenburg, Sweden
[4] School of Chemical Science and Engineering, Fibre and Polymer Technology, KTH Royal Institute of Technology, SE-100 44 Stockholm, Sweden
[5] Department of Electrical Engineering, Universidad Nacional de Colombia, Bogota, Colombia

**E-mail:** marley@kth.se

**Keywords:** Nanofluids, Electric conduction, Streamers, Dielectric liquids

OPEN ACCESS

RECEIVED
1 February 2021

REVISED
15 March 2021

ACCEPTED FOR PUBLICATION
26 March 2021

PUBLISHED
13 April 2021



## Abstract

The electric conduction under intense electric fields (up to $\sim 10^9$ V/m) in nanofluids using surface-modified ZnO–$C_{18}$ nanoparticles dispersed in mineral oil as host, is investigated with both experiments and numerical simulations. The measurements are used to estimate unknown parameters necessary to represent the generation and loss of electrons in an electrohydrodynamic model for mineral oil with and without ZnO–$C_{18}$ nanoparticles in a needle-plane configuration. The model suggests that ZnO–$C_{18}$ nanoparticles induce an enhanced field emission from negative needles, explaining the significantly larger conduction currents measured in the nanofluid compared with those in the host liquid. It is also found that the scavenging of electrons by ZnO–$C_{18}$ nanoparticles is a process which is negligible compared with the loss of electrons due to attachment in mineral oil. It is shown that ZnO–$C_{18}$ nanoparticles hinder the streamer initiation process by reducing the effective electric field at the tip of the needle. This electric field reduction is caused by the combined effect of enhanced electron injection through ZnO–$C_{18}$ nanoparticles and strong electron attachment in mineral oil. Thus, the electric field on the needle tip reaches the same threshold value when the streamer is incepted in the nanofluid as in mineral oil, although at a larger voltage. Solid evidence indicating that the additional electron scavenging and the reduced electron mobility introduced by nanoparticles has no effect in the conduction currents and in the negative streamer inception in the tested ZnO–$C_{18}$ nanofluids is shown.

## 1. Introduction

Interest in the study of nanofluids has been recently motivated by the current need to improve dielectric systems to meet the continuously increasing demands of the power industry. Several studies have shown that nanofluids produce a significant enhancement of the insulating properties of traditional dielectric liquids commonly used in electric power apparatus [1]. Thus, it has been vastly demonstrated that the addition of some nanoparticles increase the breakdown strength of mineral oil under very different experimental conditions [2–4]. The obtained dielectric improvements of nanofluids have been found to depend on several factors, such as the type, surface modification, concentration of the dispersed nanoparticles, and the moisture content of the liquid [4]. Unfortunately, theoretical assessment of the effect of the suspension of nanoparticles in mineral oil has been difficult since the fundamental physical mechanisms of electrical breakdown in dielectric liquids and their associated nanofluids are still not well understood [5].

Electric breakdown in dielectric liquids is the consequence of the initiation and development of the so-called streamers [6]. Streamers are filamentary, branched gaseous channels forming in the liquid under the influence of an applied electric field, which form a conducting path that may bridge the gap between two electrodes. Despite

of the large number of studies available in the literature, the processes involved in the initiation and development of streamers in hydrocarbons such as mineral oil are not yet fully understood [6, 7]. It has been shown that the presence of a gas cavity is required in order to initiate a positive streamer from an anode electrode [6, 8]. This process depends on the pressure externally applied to the liquid. However, there is currently no physical mechanism capable to explain the formation of such a cavity in the liquid phase [6]. On the other hand, streamer initiation at the cathode (negative streamer) is always preluded by a current pulse in the liquid. This process is not dependant upon neither the pressure nor the temperature of the liquid [8, 9]. Therefore, negative streamers are considered to be caused by electronic processes taking place in the liquid.

There are several hypotheses presented in the literature explaining the enhancement of the breakdown strength of mineral oil when nanoparticles are added [10–12]. One hypothesis suggests that hydrophilic nanoparticles improve the dielectric strength of the host liquid by adsorbing moisture [10, 13–16]. Recent experimental results show that this hypothesis is consistent only for positive streamer initiation [17]. Hydrophylic nanoparticles have however no effect on negative streamer initiation, which is unaffected by moisture content [18]. A second hypothesis suggests that nanoparticles improve the dielectric strength of the liquid by trapping electrons and converting them into slower charge carriers. According to this hypothesis, nanoparticles will effectively scavenge electrons only if they electrostatically relax within a period shorter than the time scale associated to the streamer initiation and development processes [12, 19]. Experiments have shown that nanoparticles with short relaxation time increase the voltage necessary to initiate negative streamers [17]. A third hypothesis suggests that nanoparticles improve the dielectric strength by increasing the density of shallow traps in the liquid [11, 20]. Assuming that electronic transport in the liquid mainly occurs by electron hopping processes, the increase in shallow trap density therefore leads to slower electrons [21]. This hypothesis is related to similar processes described in polymer nanocomposite dielectrics [22]. A partial correlation between improvements in positive breakdown voltage by nanofluids with higher trap density has been reported in the literature [11]. Nevertheless, no direct experimental evidence have been reported until now to clearly demonstrate the causal effect of the increase in trap density on the breakdown strength enhancement when some types of nanoparticles are added to mineral oil. Furthermore, several doubts have been cast upon this hypothesis [18].

Currently, improvements in the streamer initiation and propagation, partial discharge inception or breakdown voltages measured when nanoparticles are added to mineral oil have been correlated to the different hypotheses discussed above [5]. Unfortunately, such correlations are not sufficient to conclusively prove a cause-and-effect relationship with any hypothesis. The main challenge is that these hypotheses are directly related to microscopic electronic mechanisms induced by nanoparticles in the liquid, which cannot be assessed by experimental tests also affected by other larger-scale processes. Since electric conduction measurements in needle-to-plane configuration are only caused by high-field electronic processes in the liquid phase, they can potentially provide quantitative information to assess the validity of the existing hypotheses under negative polarity. Electrical conduction measurements in nanofluids have been recently reported [23, 24]. However, these measurements were analysed using simple analytical approaches that have serious limitations as they neglect the mutual interaction of different electrohydrodynamic processes taking place in the liquid [5]. Recently, electrical conduction measurements have been analysed through computer simulation to deduce fundamental processes in cyclohexane and mineral oil [5, 25]. There, detailed electrohydrodynamic simulations under stationary conditions were used to successfully estimate the contribution of different electronic processes from measured conduction currents.

Following a similar methodology as in [5], the electronic processes in the host liquid are here first obtained from conduction currents measured in mineral oil for a needle-plane electrode configuration under both polarities. Then, the electric conduction current is measured and simulated after nanoparticles are added to mineral oil under negative polarity. In this way, the enhanced injection of electrons due to the presence of nanoparticles is numerically estimated from the measurements. The electrostatic conditions prior to streamer initiation in ZnO–$C_{18}$ nanofluids and the host liquid are also assessed with the model. The electron scavenging and shallow trap hypotheses are analysed and discussed based on the measurement and simulated results.

In the paper, section 2 presents the experimental procedure implemented. Section 3 introduces the numerical model used. The additional processes introduced by the presence of nanoparticles are discussed in section 3.2, where a new analytical formulation for the electron scavenging process is proposed. Section 4 summarizes the obtained experimental and numerical results. Finally, the electric conduction processes just before streamer inception from negative needle are simulated in section 4.4.

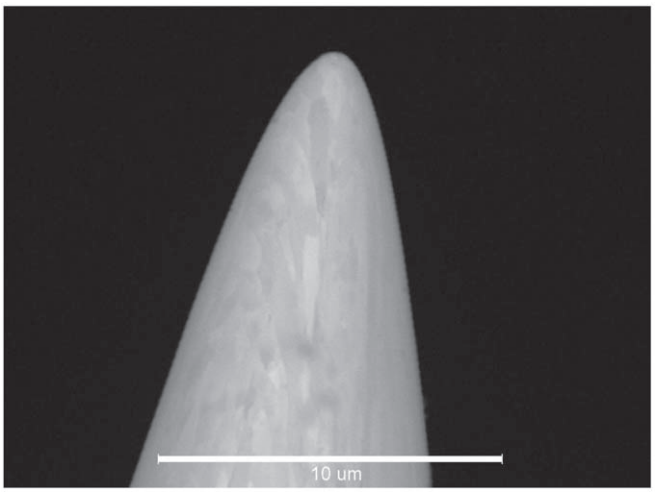


**Figure 1.** SEM image of the used needle.

## 2. Experimental procedure

The experiments are performed using a needle-plane electrode configuration in a vacuum-tight reactor as previously reported in [5, 26]. The gap distance between the plane and the tungsten needle is here set to $d_{gap} = 830$ $\mu$m. Figure 1 shows the scanning electron microscope (SEM) image used to characterize the used needle shape. A hyperbolic approximation of the contour of the image is used to define the needle geometry in the simulation. The tip radius of the needle defined as the radius at the vertex of the best-fitted hyperbola is estimated as $R_{tip} = 550$ nm.

Nitro 10NX mineral oil is used as received after filtering and degassing for 24 hours through a vacuum tight circulation path. This liquid is a mix of naphthenic, paraffinic and aromatic hydrocarbons, commonly used as transformer oil. It is a low viscosity oil containing mainly naphthenic and paraffinic molecules and having an aromatic content of 6 % [27].

The nanofluid is prepared using the procedure described in [17]. High-purity ZnO nanoparticles with a narrow size distribution centered at 20nm are synthesized by an aqueous precipitation method, and then surface-coated with octadecyltrimethoxysilane as described in [28]. This coating renders the nanoparticle surface hydrophobic and improves the stability of the nanofluid without adding additives (surfactants) into the liquid. Thus, the hydrophobic and mesoporous coating directly interacts with mineral oil molecules, improving the colloidal stability while keeping the ZnO surface directly available for electron scavenging. The ZnO–$C_{18}$ nanoparticles have a short relaxation time constant of 0.1 ns when dispersed in mineral oil [17], sufficiently low as to scavenge electrons efficiently according to [19].

In contrast to existing studies measuring conduction currents at different DC voltage levels [23, 24], an exponential ramp voltage with associated time constant $\tau = 4.1$ ms and maximum voltage of 4.5kV is here applied instead. In order to obtain sufficient data for statistical analysis of the conduction current characteristic, the voltage ramp is applied at least 30 times for each tested condition. In this way, the mean value and standard deviation along the entire steady-state conduction current characteristic are measured within less than 15 minutes, minimizing the dependence of the results to nanoparticle agglommeration. The experiment is said to be under positive or negative needle when the needle is positively or negatively charged with respect to the plane electrode. The electric current flowing through the liquid is obtained as the derivative of the charge measured using the measurement technique reported in [5].

The electric conduction currents are first measured in mineral oil. These currents measured under both polarities are used as input to the numerical model described in the next section for the estimation of the electronic processes in mineral oil. Then, the oil is extracted from the set-up and used as the host liquid for the preparation of the nanofluid. The ZnO–$C_{18}$ nanoparticles with mass density $\rho_{np} = 5610$ kg/m$^3$ are dispersed into the oil without any surfactant by using an ultrasonic bath for 30 min. The first prepared nanofluid (NFa) having a mass fraction concentration of 0.01 wt% is inserted into the set-up and the electric conduction currents are measured a second time. Then, the nanofluid is extracted from the set-up and more ZnO–$C_{18}$ nanoparticles are added until a second mass fraction concentration of 0.05 wt% is reached. The nanoparticles are dispersed in the oil by using the ultrasonic bath for additional 30 min. This second nanofluid (NFb) is inserted into the set-up and the electric conduction currents are measured a third time. Even though the measurements are also

performed under both polarities in the nanofluids, only the negative conduction current characteristic is here reported and used for the analysis of the electronic processes in the presence of nanoparticles as it will be described in the next section.

Dynamic light scattering measurements with a 633 nm He/Ne laser at 25 deg C show that the nanofluid is stable during the testing period. However, some agglomeration of the nanoparticles have been detected after preparation when increasing nanoparticle concentration. Thus, formation of clusters with primary particle radius distribution centred at 75 and 190 nm are measured for the nanofluids NFa and NFb respectively [17].

## 3. Numerical model

The simulation of the conduction currents in the tested configuration is performed by implementing the self-consistent electro-hydrodynamic (EHD) model for mineral oil reported in [5]. This model includes the electrohydrodynamic motion of the liquid to take into account its effect on the conduction current [25]. In addition, the model is extended to include the additional processes introduced by the dispersed nanoparticles. Thus, the charge continuity equations and Poisson equation:

$$\frac{\partial n_e}{\partial t} + \nabla \cdot (n_e \mathbf{W}_e - D_e \nabla n_e) = \frac{G_I}{e} + \alpha_{imp} n_e W_e - \eta_{att} n_e W_e - S_{np} - R_{e.p}\, n_e\, n_p, \tag{1}$$

$$\frac{\partial n_n}{\partial t} + \nabla \cdot (n_n \mathbf{W}_n - D_n \nabla n_n) = \eta_{att} n_e W_e - R_{p.n}\, n_n\, n_p, \tag{2}$$

$$\frac{\partial n_{np}}{\partial t} + \nabla \cdot (n_{np} \mathbf{W}_{np} - D_{np} \nabla n_{np}) = S_{np} - R_{np.p}\, n_{np}\, n_p, \tag{3}$$

$$\frac{\partial n_p}{\partial t} + \nabla \cdot (n_p \mathbf{W}_p - D_p \nabla n_p) = \frac{G_I}{e} + \alpha_{imp} n_e W_e - R_{p.n}\, n_n\, n_p - R_{np.p}\, N_n\, n_p - R_{e.p}\, n_e\, n_p, \tag{4}$$

$$\nabla \cdot \mathbf{E} = -\nabla^2 V = \frac{e(n_p - n_e - n_n - n_{np})}{\epsilon_0 \epsilon_r}, \tag{5}$$

are solved coupled with Navier–Stokes equations for a non-compressible liquid in laminar flow:

$$\nabla \cdot \mathbf{u} = 0. \tag{6}$$

$$d_L\left(\frac{\partial \mathbf{u}}{\partial t} + (\mathbf{u} \cdot \nabla)\mathbf{u}\right) = -\nabla p + \zeta \nabla^2 \mathbf{u} + e(n_p - n_n - n_{np})\mathbf{E} + \epsilon_0(\epsilon_r - 1)(\epsilon_r + 2)\nabla E^2, \tag{7}$$

where $\mathbf{E}$ is the electric field, $V$ the electric potential and $e$ the elementary charge. The number density of positive ions, negative ion and electrons are $n_p$, $n_n$ and $n_e$ respectively. $n_{np}$ is the number density of electrons scavenged by the nanoparticles. $\epsilon_0$ and $\epsilon_r$ are the vacuum permittivity and the relative permittivity of the liquid. The drift velocity of electrons, negative ions, charged nanoparticles and positive ions is $\mathbf{W}_e = -\mu_e \mathbf{E}$, $\mathbf{W}_n = -\mu_n \mathbf{E} + \mathbf{u}$, $\mathbf{W}_{np} = -\mu_{np} \mathbf{E} + \mathbf{u}$ and $\mathbf{W}_p = \mu_p \mathbf{E} + \mathbf{u}$, respectively. $\mathbf{u}$ is the velocity of the liquid, and $\mu_e$, $\mu_n$, $\mu_{np}$ and $\mu_p$ are the mobility of electrons, negative ions, nanoparticles and positive ions. The mobility of the nanoparticles is estimated with the Walden rule as $\mu_{np} = Q_{np}/(6\pi\zeta R_{np})$, where $Q_{np}$ and $R_{np}$ are the charge and radius of the nanoparticle, and $\zeta$ the dynamic viscosity of the mineral oil. $S_{np}$ is the electron scavenging term due to nanoparticles in the host liquid, detailed later in section 3.2. $D_e$, $D_n$, $D_{np}$ and $D_p$ are the diffusion coefficients for electrons, negative ions, nanoparticles, and positive ions. $R_{e.p}$, $R_{p.n}$ and $R_{np.p}$ are the electron-ion, ion-ion and nanoparticle-ion recombination coefficients. $d_L$, $\zeta$ and $p$ are the mass density, the dynamic viscosity, and the pressure of the liquid. $\epsilon_0(\epsilon_r - 1)(\epsilon_r + 2)\nabla E^2$ is the electric force exerted on the liquid [29]).

The model is solved using the finite element method (FEM) using a commercial software [30]. The electric current flowing through the electrodes is estimated using the modified Sato equation according to [31]. The parameters of mineral oil Nytro 10X assumed in the simulations are listed on table 1. Here, some improvements have been considered for the used parameters in comparison with our previous publication [5]. Particularly, the diffusion-controlled recombination coefficient is used instead since it is in better agreement with measurements of recombination in liquids (such as mineral oil) with low electron mobilities [32], in contrast to the Langevin recombination proposed in [12]. Furthermore, the positive and negative carrier mobilities of cyclohexane [25] are used instead as representative for those in mineral oil at high electric fields. However, the reader should be aware that most parameters in table 1 are not yet known in mineral oil at high electric fields and the values used here are educated estimates in the absence of sufficient experimental data [19, 33].

### 3.1. Physical processes in the host oil

A detailed simulation analysis of the conduction currents in mineral oil [5] has shown that the electron generation in the liquid can be described by using generalized equations usually attributed to two different mechanisms: Zener molecular ionization [35–37] and electron impact ionization [38–40]. Thus, the generation

**Table 1.** Parameters used in the EHD model for mineral oil.

| Parameter | Value | Source |
|---|---|---|
| $\mu_e$ | $1 \times 10^{-4}$ m$^2$/(Vs) | [12] |
| $D_e$ | $2.6 \times 10^{-6}$ m$^2$/s | [5] |
| $\mu_n$ | $1 \times 10^{-8}$ m$^2$/(Vs) | [34] |
| $\mu_p$ | $3 \times 10^{-7}$ m$^2$/(Vs) | [25] |
| $D_n, D_p$ | $6.7 \times 10^{-11}$ m$^2$/s | Calculated |
| $\epsilon_r$ | 2.2 | [5] |
| $d_L$ | 880 kg/m$^3$ | [27] |
| $\eta$ | $1.232 \times 10^{-2}$ kg/(ms) | [27] |
| $R_{ei}, R_{ii}$ | $1 \times 10^{-13}$ m$^3$/s | [32] |

of electrons by Zener molecular ionization is represented by the function $G_I$ defined as [12]:

$$G_I = A_I E \exp(-B_I/E), \tag{8}$$

where $A_I$ and $B_I$ are constants depending on the liquid. This mechanism is dominant when the needle is positively charged, with a secondary role as source of initial electrons under negative polarity [5]. In turn, the electron impact ionisation coefficient $\alpha_{imp}$ is given by [32]:

$$\alpha_{imp} = A_\alpha n_l \exp(-B_\alpha n_l/E). \tag{9}$$

with empirical constants $A_\alpha, B_\alpha$ for the liquid with number density $n_l$. This mechanism is the dominant source of electrons when the needle is negatively charged, having a minor effect under positive polarity [5].

As electrons drift, they are converted into slower negatively charged liquid molecules (negative ions) by a process known as attachment. Since attachment of electrons in mineral oil has a significant effect when the needle is negatively charged, it is here considered through the coefficient $\eta_{att}$ representing the number of electrons lost per unit length . Even though $\eta_{att}$ is not known for most hydrocarbons, it is expected to decrease at high electric fields as the electron energy exceeds the energy difference required to form a negative ion [41]. Even though the decrease of attachment at high fields could be approximated by a linear function [25], a more general approximation is here implemented. For that, the attachment coefficient is defined by piece-wise interpolation from a vector $\eta_{att}^{(j)}$ defined at three discrete electric fields $\mathbf{E}^{(j)}$ (where $j = 1, 2, 3$) as:

$$\eta_{att} = \begin{cases} C_1(E) & E^{(1)} < E < E^{(2)} \\ C_2(E) & E^{(2)} < E < E^{(3)} \end{cases} \tag{10}$$

given by a two cubic Hermite polynomial functions $C_1, C_2$ with continuous first derivatives. The electric field vector is chosen as $\{1 \times 10^5, 4 \times 10^8, 2 \times 10^9\}$ [V/m]. The limit values $E^{(1)}$ and $E^{(3)}$ in this interval are selected considering the minimum and maximum electric fields expected in the gap above the ohmic regime. The middle point $E^{(2)}$ is arbitrarily chosen as an initial guess of the critical field at which the rates of ionization and attachment are in the same order of magnitude.

Even though several values have been suggested in the literature for $A_I$ and $B_I$ in mineral oil [33, 37, 42], they do not have any theoretical or empirical justification [33] and have been shown to grossly overestimate the production of electrons in the liquid [5]. Moreover, the parameters for impact ionization and attachment $A_\alpha n_l$, $B_\alpha n_l$, $\eta_{att}^{(1)}$, $\eta_{att}^{(2)}$ and $\eta_{att}^{(3)}$ in equations (9) and (10) are not known for mineral oil. As in [5], all these parameters describing the generation and loss of electrons in the host liquid are here tuned until the simulated conduction currents best fit the corresponding measured currents in mineral oil. However, the search for these parameters is here implemented instead as an inverse optimization problem. Thus, the parameters $A_I, B_I, A_\alpha n_l, B_\alpha n_l, \eta_{att}^{(1)}, \eta_{att}^{(2)}$ and $\eta_{att}^{(3)}$ are simultaneously solved as optimization variables that minimize the least square error between the measured and calculated logarithm of the conduction currents under both polarities. The optimization is performed using the derivative-free Nelder-Mead method [43].

### 3.2. Additional electronic processes when nanoparticles are suspended

Once the parameters used to represent the generation and loss of electrons are obtained for mineral oil, they are assumed to remain unaffected when nanoparticles are added. Observe that even though nanoparticles dispersed in the oil intensify the electric field around them [19], this local effect will lead to a negligible increase in the generation of electrons in the liquid. Since this field enhancement vanishes rapidly within a fraction of the nanoparticle radius, no significant impact or Zener ionization is possible within such a short distance. Thus, the

simulation of conduction process in the nanofluid under negative polarity is performed considering additional processes to those already included in the previous subsection.

Even though measurements have showed that the cold field emission is not a relevant conduction mechanism in mineral oil for sharp needles [5], there is experimental evidence that the presence of ZnO nanostructures enhance electron injection [44]. Moreover, it has been shown that nanoparticles tend to stick to the needle tip enhancing its electric field [23]. Thus, single or agglomerated nanoparticles standing on the needle surface can induce enhanced field emission leading to an increased electron current density $J_e$ at the cathode boundary, defined as [45]

$$J_e = \frac{a_{FN}(\beta E)^2}{\phi} \exp\left(-\frac{\nu(f) b_{FN} \phi_{liq}^{1.5}}{\beta E}\right), \tag{11}$$

where $a_{FN} = 1.54 \times 10^{-6}$ A eV V$^2$ and $b_{FN} = 6.83 \times 10^9$ eV$^{-1.5}$ V m$^{-1}$ are the first and second Fowler-Nordheim parameters. The correction factor $\nu(f)$ and the scaled barrier field $f$ are defined as

$$\nu(f) = 1 - f + 0.166 f \ln(f) \tag{12}$$

$$f = \frac{e^3(\beta E)}{4\pi\epsilon_0 \epsilon_r \phi_{liq}^2} \tag{13}$$

The parameter $\phi_{liq}$ is the apparent work function defined as the difference of the work function of the emitting surface $\phi$ and the energy of the bottom conduction band in the liquid $\Delta\phi$ measured from the vacuum level [46]. Unfortunately, $\phi$ for the tested ZnO nanoparticles is not yet known. However, there is experimental evidence that the work function measured in ZnO films with organic ligands (such as the octadecyltrimethoxysilane (C18) here used) on metal surfaces is significantly lower than the work function of pure ZnO of about 4.8eV [47]. Similarly, $\Delta\phi$ for mineral oil is not known, although it should range between 0 and −0.6 eV by comparison with other hydrocarbons with similar electron mobility [5]. Considering the existing uncertainities, an apparent work function $\phi$=4eV is here assumed. The parameter $\beta$ is the field intensification factor representing the local increase in electric field on the surface of the needle caused by an emitting single nanoparticle or an agglomerated cluster [12, 19]. Since $\beta$ is difficult to measure or estimate, it is usually taken as a fitting factor [48]. Here, $\beta$ is optimized until a good agreement between the simulated and measured conduction current in the nanofluids under negative polarity is reached considering an emitting nanoparticle agglomerate with the measured mean primary cluster radius [17].

On the other hand, electrons drifting towards uncharged, dielectrically relaxed nanoparticles can be readily converted into slow negatively charged nanoparticles [12]. In the literature, this additional electron scavenging process has been analytically modelled through a time constant $\tau_{np}$ [12, 19]. The lowest possible value of $\tau_{np}$ for conducting nanoparticles is 2ns [12]. However, this approach grossly misestimates the electron scavenging caused by nanoparticles [18]. Therefore, the electron scavenging process is modelled in this work following [18], where a different analytical expression is derived to represent this process. There, the temporal rate of change of the charge $Q(t)$ of a single nanoparticle due to electron scavenging is defined as [12, 19]:

$$\frac{dQ(t)}{dt} = \frac{3Q_s}{\tau_{pc} A(t)} \left[\frac{Q(t)}{Q_s} - \frac{A(t)}{3}\right]^2, \tag{14}$$

where the squared term on the right hand side of (14) reflects the reduction in $dQ(t)/dt$ as the limit of electrons than can be trapped by a nanoparticle is reached. Thus, $Q_s$ is the electron saturation charge for the nanoparticle given by

$$Q_s = 12\pi\epsilon_{oil} R_{np}^2 E, \tag{15}$$

$\epsilon_{oil}$ is the electric permittivity of the host oil and $R_{np}$ is the radius of the nanoparticle. $\tau_{pc}$ is the time constant for nanoparticle charging defined as

$$\tau_{pc} = \frac{4\epsilon_{oil}}{e n_e \mu_e}, \tag{16}$$

where $e$ is the elementary charge, $n_e$ is the number density of electrons present in the nanofluid, and $\mu_e$ is the electron mobility. The variable $A(t)$ is:

$$A(t) = 1 + 2\frac{\epsilon_{np} - \epsilon_{oil}}{2\epsilon_{oil} + \epsilon_{np}} \exp\left(-\frac{t}{t_r}\right) + 2\frac{\sigma_{np} - \sigma_{oil}}{2\sigma_{oil} + \sigma_{np}} \left[1 - \exp\left(-\frac{t}{t_r}\right)\right]. \tag{17}$$

$\epsilon_{np}$ is the electric permittivity of the nanoparticle. $\sigma_{oil}$ and $\sigma_{np}$ are the electric conductivity of the oil and the nanoparticle, respectively. $\tau_r$ is the charge relaxation time constant of the nanoparticle given by:

$$\tau_r = \frac{2\epsilon_{oil} + \epsilon_{np}}{2\sigma_{oil} + \sigma_{np}}. \tag{18}$$

In the case of a ZnO nanoparticle, $\tau_r \approx 10$ ps [19], which is significantly lower than the time scales associated to the conduction processes in mineral oil [5]. This short relaxation time also allows treating ZnO as a highly conducting nanoparticle with the electrical conductivity $\sigma_{np}$ more than 10 orders of magnitude larger than $\sigma_{oil}$ [19]. Therefore, $A(t) \approx 3$ and the nanoparticle charging rate $dQ(t)/dt$ in equation (14) becomes

$$\frac{dQ(t)}{dt} = \frac{Q_s}{\tau_{pc}}\left(\frac{Q}{Q_s} - 1\right)^2. \tag{19}$$

The electron scavenging source term $S_{np}$ due to the presence of all nanoparticles dispersed in a host liquid with volumetric mass density $\rho_{oil}$ in equations (1) and (3) is thus [18]

$$S_{np} = \frac{N_{np}}{e}\frac{dQ(t)}{dt}, \tag{20}$$

where $N_{np}$ is the number density of the nanoparticles dispersed in the host liquid, defined as $3\ k_m \rho_{oil} / (4\pi R_{np}^3 \rho_{np})$ for nanoparticles with radius $R_{np}$, mass fraction concentration $k_m$ (i.e. 0.01 wt% for NFa and 0.05 wt% for NFb) and volumetric mass density $\rho_{np}$. If agglomeration occurs in the nanofluid, $N_{np}$ should be estimated using the mean radius of the measured clusters instead of the radius of a single nanoparticle.

Then, the scavenging source term $S_{np}$ can be rewritten by combining equations (15) and (16) into (20) as:

$$S_{np} = n_e\left[\ 3\ N_{np}\ R_{np}^2\ \mathbf{W}_e\left(\frac{e\ n_{np}}{(12\ \pi\ R_{np}^2\ \epsilon_{oil}\ E) N_{np}} - 1\right)^2\ \right]. \tag{21}$$

In addition to the processes above, the electron mobility $\mu_e$ has also been suggested to change when nanoparticles are dispersed in mineral oil [11]. It has been hypothesed that nanoparticles create additional shallow traps of less than 0.5eV in which electrons get captured and then released. This trapping and detrapping process of electron transport would lead to a decrease of the electron mobility of the nanofluid in relation to the host liquid. Up to now, only indirect estimates using electron hoping theory predict a reduction of the electron mobility of $Al_2O_3$, $TiO_2$ and $Fe_3O_4$ nanofluids of less than 43% compared with mineral oil [11]. Since the chosen electron mobility of the ZnO nanofluid does not affect the simulated conduction currents, even for $\mu_e$ as low as half of that in the host liquid, the same value in table 1 is used in the simulations. Similarly, the presence of nanoparticles have also been reported to influence the ion mobilities in mineral oil [49, 50]. However, such measurements have been only made at low electric fields for $TiO_2$ and ferro nanofluids and no data are available about the change of the ionic mobilities in mineral oil when ZnO nanoparticles are used. Thus, the ionic mobilities in the nanofluid are also here taken as those of the host liquid.

## 4. Results

### 4.1. Conduction currents in mineral oil

Current-voltage (IV) characteristics measured in dielectric liquids are generally classified within three different regimes [5, 18]: ohmic, injection/generation, and space charge limited. At low electric fields in the ohmic regime, the current increases linearly with applied voltage due to the presence of ionic charges in the liquid. As the electric field increases, the measured current increases exponentially with applied voltage due to injection and/or generation of electrons, defining the second regime. At even higher electric fields, the produced ionic charges of the same polarity as the needle accumulate in front of it, creating a space charge cloud sufficiently large as to distort the electric field [18, 48]. Thus, the electric field at the tip of the needle becomes lower than the Laplacian electric field. As a consequence, the rate of increase of the conduction current with voltage starts saturating, defining the space charge limited regime.

figure 2 shows the high-field electric conduction currents measured for mineral oil under both polarities. The error bars shown represent the 68% confidence intervals defined by one standard deviation above and below the mean value. Observe that the currents in the ohmic regime are not measured since they are below the charge detection threshold in the experiment. Analysis of the measured negative currents using the widely-used Fowler-Nordheim plot ($\ln(I^2/V)$ as a function of $V^{-1}$) [48] shows that the characteristic yields a straight line for voltages lower than about 3300V. This range corresponds to the generation regime in mineral oil, which is dominated by Zener molecular ionization and electron impact ionization rather than by electron field emission (as demonstrated in [5]). At higher voltages, the space-charge limited behavior is observed for the negative needle (such that $I^{0.5}$ varies linearly with V [48]). On the other hand, the Halpern-Gomer plot ($\log_{10}(I)$ as a function of $V^{-1}$) [51] of the positive characteristic shows that the measured currents in that polarity correspond mainly to

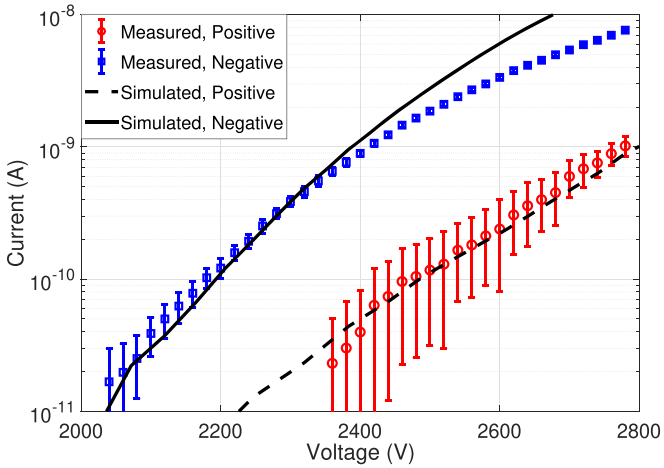


**Figure 2.** Current voltage characteristics in mineral oil with positive and negative needle. The currents estimated with the model are also included. The error bars correspond to the standard deviation above and below the mean value.

**Table 2.** Optimization variables estimated with the EHD model for mineral oil and for ZnO–$C_{18}$ nanofluids.

| Process | Parameter | Value | Units |
|---|---|---|---|
| Molecular ionization (host liquid) | $A_I$ | $2.28 \times 10^2$ | $S/m^2$ |
| | $B_I$ | $6.1 \times 10^9$ | V/m |
| Electron impact ionization (host liquid) | $A_\alpha n_l$ | $1.9 \times 10^7$ | $m^{-1}$ |
| | $B_\alpha n_l$ | $1.474 \times 10^8$ | V/m |
| Electron attachment (host liquid) | $\eta_{att}^{(1)}$ | $1.63 \times 10^7$ | $m^{-1}$ |
| | $\eta_{att}^{(2)}$ | $1.00 \times 10^7$ | $m^{-1}$ |
| | $\eta_{att}^{(3)}$ | $4.26 \times 10^5$ | $m^{-1}$ |
| Enhanced field emission (nanofluid) | $\beta$ | 3.75 (NFa), 3.83 (NFb) | |

the space-charge limited regime. The positive characteristic has also larger confidence intervals compared with the negative case as the currents under positive needles in mineral oil are noisy and are much less reproducible as observed in experiments with other hydrocarbons [48].

The conduction currents simulated for mineral oil using the same voltage waveform applied in the experiment are also shown in figure 2. As can be seen, the agreement is excellent between the simulations and the measured currents in positive polarity. Similarly, the simulated currents match well those measured for negative polarity in the generation regime, although with increasing differences at higher voltages in the space charge limited zone. This result is expected as the simulated space-charge-limited currents can be overestimated at higher voltages due to the model assumption of a laminar electrohydrodynamic flow. Observe that the liquid motion is likely to change from laminar into a unsteady flow, such that turbulence losses (not accounted in equation (7)) increase, making the removal of accumulated charges less efficient as reported in cyclohexane [25].

The optimization variables $A_I$, $B_I$, $A_\alpha n_l$, $B_\alpha n_l$, $\eta_{att}^{(1)}$, $\eta_{att}^{(2)}$ and $\eta_{att}^{(3)}$ found to best fit the experimental data in the experiment with mineral oil are listed in table 2. Observe that differences are found between the optimized values for these variables and those reported in [5]. These differences are attributed to the simultaneous solution of the unknown parameters and to the better transport parameters used here for mineral oil (table 1). Note that the set of optimization variables here obtained to describe the generation and loss of electrons in mineral oil is not unique and is only valid in connection with the other parameters used in the simulation and summarized in table 1. Thus, the entire simulation model with the obtained optimization variables is self-consistent to reproduce the measured electrical conduction processes in mineral under similar conditions as those tested here. Since the variables in table 2 are not obtained through direct measurements of electron production or loss, their value should be considered as intermediate estimates consistent at least with the conduction measurements here reported. Although not unique, this set is here used as the best possible way to quantitatively evaluate the microscopic processes in mineral oil, in the absence of direct measurements of charge transport and electron production/loss parameters at high fields.

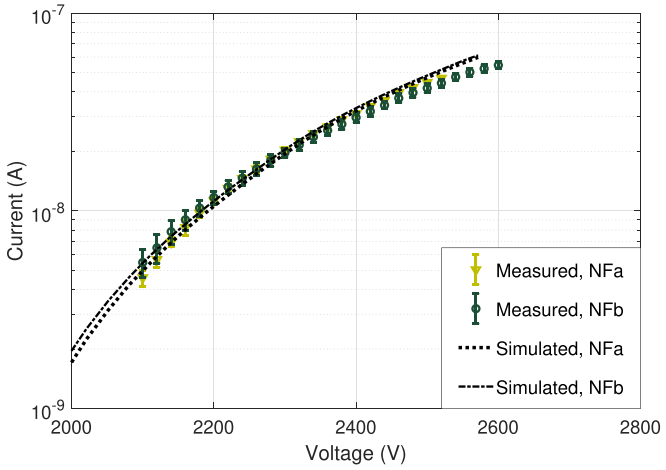


**Figure 3.** Current voltage characteristics with negative needle in mineral oil based ZnO–$C_{18}$ nanofluids synthesized at 0.01 wt% (NFa) and 0.05 wt% (NFb) mass fraction concentrations. The currents estimated with the EHD model are also included. The error bars correspond to the standard deviation above and below the mean value.

### 4.2. Negative conduction currents in ZnO nanofluids

Since the additional electronic processes influencing the electric conduction for nanofluids (as described in section 3.2) are relevant mainly for negative needles [5], only results obtained with this polarity are here analysed. Figure 3 shows the electric conduction currents measured with negative needle for ZnO–$C_{18}$ nanofluids at 0.01 wt% (NFa) and 0.05 wt% (NFb) at high electric fields of up to $10^9$ V/m (at the needle tip). Analysis of the currents measured for the used nanofluids with Fowler-Nordheim plots (not shown here) indicate that the injection/generation regime occurs for voltages lower than 2500 V with the space charge limited regime at larger voltages. These conduction currents measured for both tested nanofluids are more than an order of magnitude larger than for the host liquid (shown in figure 2). This increased conduction current in nanofluids compared with the host liquid is consistent with previous measurements [23, 24, 26]. On the other hand, only a slightly larger conduction current is measured at lower voltages for the nanofluid with larger nanoparticle concentration (NFb). However, there are only minor overall differences between the measured currents $I_{NFa}$ and $I_{NFb}$ under the two tested nanoparticle concentrations.

The negative conduction currents simulated including the enhanced electron injection and the electron scavenging effect due to the presence of the nanoparticles (as described in section 3.2) are also shown in figure 3. As expected, there is a good agreement between the simulation and the measurements in the injection/generation regime. Nevertheless, in a similar manner as for the host liquid, the estimated currents in the nanofluid are slighly larger than those measured in the space-charge limited regime due to the assumption of laminar liquid flow. The optimized field intensification factor $\beta$ found for the nanofluid NFa is 3.75, only 2% smaller than the case with a larger nanoparticle concentration in NFb, as indicated in table 1. This minor change in $\beta$ suggests that the enhanced electron injection is weakly dependent on the nanoparticle concentration within the tested range (0.01-0.05wt%). This result supports the assumption here taken that a single ZnO cluster agglomerate occupies the entire high electric field zone at the needle tip. Therefore, this cluster agglomerate emit electrons with nearly the same current density regardless of the concentration of nanoparticles in the liquid bulk.

### 4.3. Electronic processes in the mineral-oil-based ZnO–$C_{18}$ nanofluid under the tested experimental conditions

Once all the unknown model parameters are estimated from the conduction current measurements, the physical processes involved in the conduction currents in the mineral-oil-based ZnO–$C_{18}$ nanofluid can be quantified up to electric fields of $1 \times 10^9$ V/m. Figure 4 shows the frequency of the different processes of generation and loss of electrons in the tested nanofluid, estimated by the model using the optimized parameters in table 1. As can be seen, the frequency of collisional ionization $\nu_{ioniz}$ (defined as $\alpha_{imp} W_e$) and of attachment $\nu_{attach}$ (given by $\eta_{att} W_e$) in the host oil dominate the production and loss of electrons in the nanofluid. According to figure 4, avalanches can develop in mineral oil and its derived nanofluids at local electric fields larger than a critical value $E_s$ of about $3 \times 10^8$ V/m, granted that initial electrons are available. Under such a condition, electrons can multiply since the rate of their production is higher than for their loss (i.e $\nu_{ioniz} \geqslant \nu_{attach}$). Observe that the estimated $E_s$ in mineral oil is larger than that found in cyclohexane (of $2 \times 10^8$ V/m) [39]. This result is consistent with the experimental fact that the inception of negative streamers in mineral oil takes place at larger voltages than in cyclohexane [52].

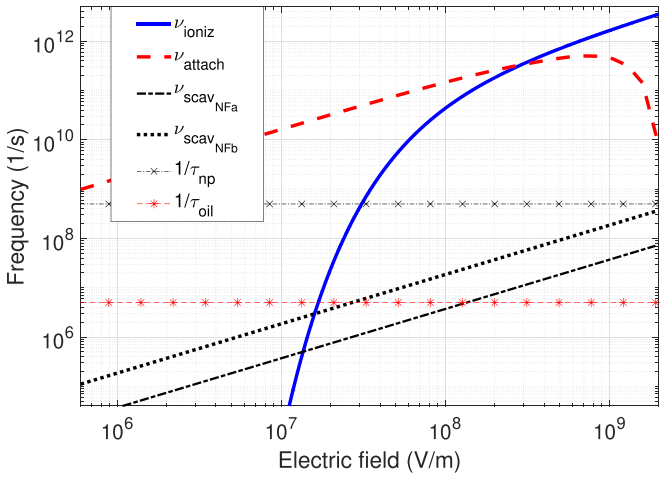


**Figure 4.** Frequency of different electronic processes estimated from the high-field conduction currents in mineral oil based ZnO–$C_{18}$ nanofluids. The frequencies for attachment and scavenging based on the time constants $\tau_{oil}$ and $\tau_{np}$ generally used in the literature are also included for sake of comparison.

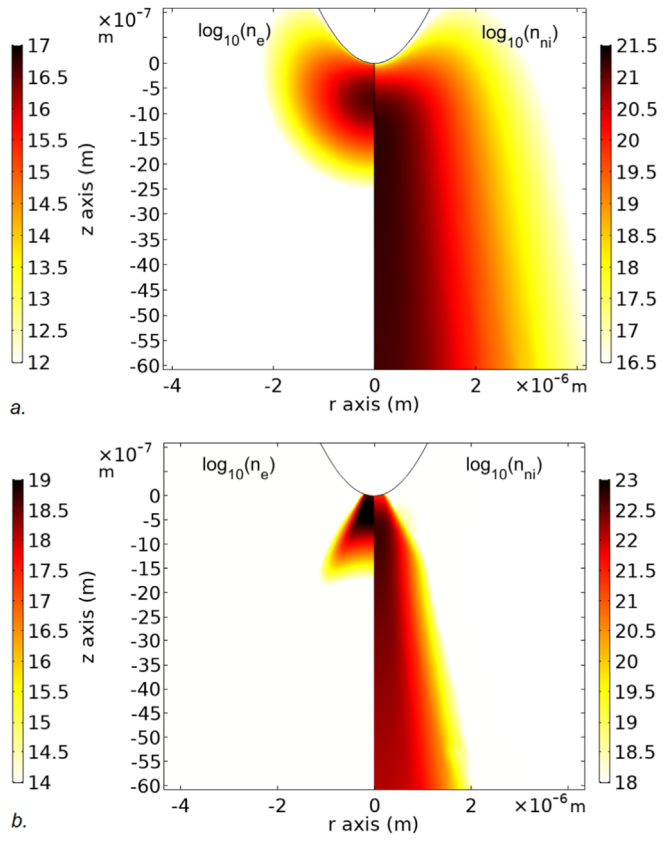


**Figure 5.** Surface plot of the logarithm of the density (in $m^3$) of electrons $n_e$ (left) and negative ions $n_{ni}$ (right) in front of the needlepoint at 3000V for a) mineral oil and b) ZnO–$C_{18}$ nanofluid NFb.

A representative example of the spatial density distribution of electrons and negative ions, mainly produced by ionization and attachment processes, is shown in figure 5 in mineral oil and in the nanofluid at a voltage level of 3000 V. In this case, electron avalanches develop within the first few micrometres from the electrode tip in both cases, before they are mainly converted into negative ions by attachment. Observe that this penetration depth of the avalanches into the gap is in the same order of magnitude as estimated for other hydrocarbons [48]. It is noteworthy however, that the avalanche penetration depth is not related to the tip radius as previously suggested [53]. Instead, it is defined by the location where the total field (including the space charge shielding) reaches $E_s$ and by the additional attachment distance required to reduce significantly the size of the drifting electron avalanche after

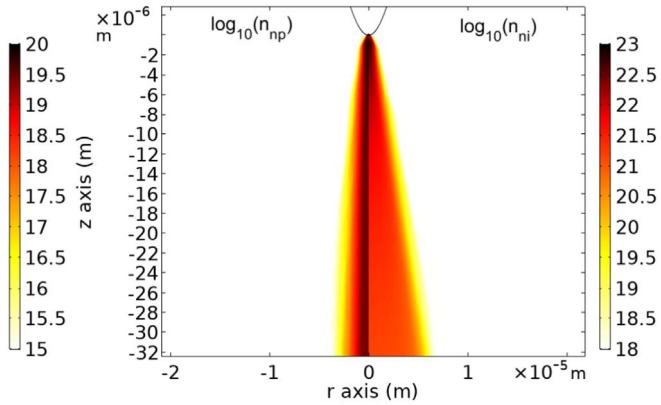


**Figure 6.** Surface plot of the logarithmic density (in $m^3$) of electrons scavenged by nanoparticles $n_{np}$ (left) and negative ions $n_{ni}$ (right) in the gap at 3000V for the ZnO–$C_{18}$ nanofluid NFb.

it stops multiplying. These avalanches are started by a low density of initial electrons produced by Zener molecular ionization over a submicrometric thin layer of high electric field ($E > 1 \times 10^8$ V/m) on the needle tip. In the presence of nanoparticles, enhanced field injection from the needle tip causes a significant flux of initial electrons which, after multiplying, reach a maximum density more than two orders of magnitude larger than in mineral oil. As negative ions are slower than electrons, they accumulate and reach densities more than three orders of magnitude larger than those of electrons. Observe that the extension of the charged plumes in figure 5 are defined by the strong coupling between the velocity field induced by the EHD motion and the electrostatic forces due tot he injected carriers as observed in other liquids under the high field conduction regime [25].

Interestingly, the frequency of electrons scavenged by the ZnO-$C_{18}$ nanoparticles dispersed in the liquid $\nu_{scaven}$ (the term within the square parenthesis in equation (21)) also shown in figure 4, is more than three orders of magnitude lower than the attachment frequency $\nu_{attach}$. This result demonstrates that even though nanoparticles may scavenge electrons, the frequency of this process is negligible compared with the already existing high loss of electrons due to attachment in the host liquid. This is also evident for instance by comparing the logarithmic distribution of the density of electrons scavenged by the nanoparticles $n_{np}$ and of electrons attached into negative ions $n_n$ as shown in figure 6 for the NFb nanofluid at 3000 V. In this case, $n_{np}$ is more than three orders of magnitude smaller than $n_n$ in the close proximity of the rod. As the plume of negative ions and negatively charge nanoparticles moves along the hydrodynamic flow, the magnitude of $n_{np}$ and $n_n$ starts decreasing away from the needle. However, the significantly lower density of $n_{np}$ compared with $n_n$ is still maintained all along the entire gap.

The above-described low frequency of electron loss due to the presence of ZnO-$C_{18}$ nanoparticles compared with electron attachment in the host fluid is an important finding that challenges the widely-spreading electron scavenging theory of nanoparticles [12, 19]. Observe that the zero-field attachment time constant $\tau_{att} = 200$ ns for mineral oil was conveniently assumed to justify this theory in [12, 19], a value which was much larger than the estimated scavenging time constant $\tau_{np} = 2$ ns for conducting nanoparticles. Consequently, this theory was justified by assuming that the scavenging frequency due to nanoparticles $1/\tau_{np}$, also shown in figure 4, is two orders of magnitude larger than the assumed frequency of electron attachment in the liquid $1/\tau_{att}$. However, observe that the zero-field attachment frequency $1/\tau_{att}$, widely used for mineral oil (e.g. [19, 54, 55]), is more than four orders of magnitude smaller than the actual high-field attachment frequency $\nu_{attach}$ here estimated from the measurements. This fact also casts doubts on the simulation of negative streamers using the zero-field attachment constant $\tau_{att}$ (as in [56]), which would exaggerate the penetration depth of avalanches in the liquid.

### 4.4. Conditions prior to negative streamer inception in ZnO–$C_{18}$ nanofluids

Since negative streamers are initiated by electronic processes in the liquid [57], the model could also be used to shed light upon the mechanisms involved. Given that no streamers are initiated in the experiment described above, the model is here implemented to reproduce the testing conditions described in [17]. In this experiment, it was observed that the voltage required to initiate negative streamers in ZnO–$C_{18}$ nanofluids is significantly larger than in mineral oil and it was also weakly sensitive to the nanoparticle concentration (up to 0.05 wt%). The tip radius of the negatively charged needle was $R_{tip} = 225$ nm, separated by a distance $d_{gap} = 4.5$ mm from a sphere electrode. A voltage ramp with a rate of about $2.75 \times 10^9$ V/s was applied to the sphere while the needle was grounded.

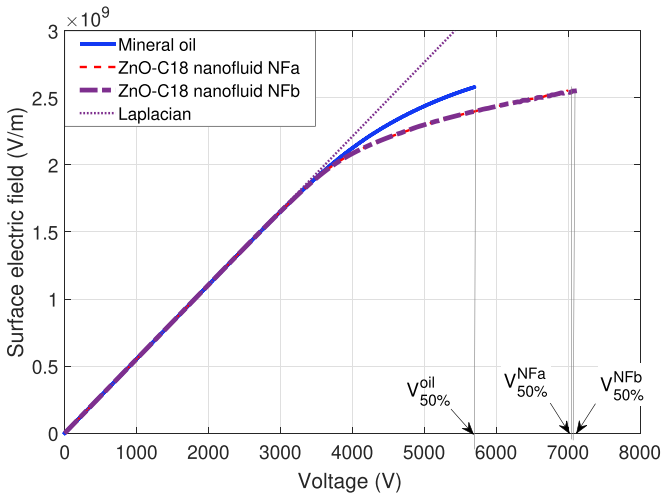


**Figure 7.** Negative surface electric field $E_{tip}$ at the needle tip in mineral oil and in the ZnO–$C_{18}$ nanofluids NFa and NFb. The Laplacian electric field $E_{lap}$ is also shown as reference. The corresponding 50% probability of streamer inception voltage $V_{50\%}$ is also indicated.

figure 7 shows the simulated electric field $E_{tip}$ at the tip of the needle as a function of the applied voltage in mineral oil without and with ZnO–$C_{18}$ nanoparticles. The corresponding Laplacian electric field $E_{lap}$ at the tip of the needle is also included as a reference. The 50% probability negative streamer inception voltage $V_{50\%}$ measured in the host liquid and the nanofluid in [17] is also indicated.

As expected, the effective tip electric field $E_{tip}$ (including the shielding effect of the space charge accumulated in front of the needle) in both cases starts deviating from the laplacian electric field $E_{lap}$ at the start of their corresponding space-charge-limited injection regime. However, the enhanced field emission produced in the nanofluid leads to an intensified production of negative carriers (mainly electrons and negative ions), which produces a larger electrostatic shielding of the needle electric field compared with case of mineral oil alone. Thus, $E_{tip}$ in the nanofluid is lower than in the host liquid at voltages in the space-charge limited regime.

As the voltage further increases, the threshold field $E_{str}$ on the needle surface at which streamers are initiated in mineral oil at the measured $V_{50\%}$ of 5696 V [17] is estimated at about $2.5 \times 10^9$ V/m. At that voltage level, $E_{tip}$ in the nanofluid case is still 20% lower than in the host fluid due to the strong space charge shielding induced by enhanced field emission. Thus, the applied voltage in the nanofluid needs to further increase to 7111 and 7157 V in order to initiate streamers in the nanofluids NFa and NFb respectively [17]. Interestingly, the estimated streamer threshold field $E_{str}$ in the nanofluids is then nearly the same as in the host liquid, regardless of the tested nanoparticle concentration (0.01 or 0.05 % wt). The fact that the estimated effective $E_{str}$ at the streamer inception voltage in the host liquid and in the nanofluid is roughly the same, shows that the relation between the probability of streamer initiation and the surface electric field of the stressed electrode [6, 7] also holds for sharp needles with strong space charge shielding.

Observe that the scavenging hypothesis [12, 19] would predict a stronger scavenging of electrons when increasing nanoparticle concentration, which in turn would cause a larger accumulation of charged nanoparticles electrostatically shielding the needle tip. Then, a larger shielding of $E_{tip}$ would lead to a higher streamer inception voltage. These predictions are however not supported by the results in figure 7 or by the nanofluid streamer inception voltages measured in [17], which are independent of the density of dispersed nanoparticles. These results show instead that the larger streamer inception voltage in ZnO–$C_{18}$ nanofluids is mainly caused by the strong production of negative carriers due to the enhanced electron injection at the cathode. This process is however only active under negative needles when there is a continuous emission of electrons from the electrode surface into the liquid through nanoparticles (as single particles or as agglomerate clusters) with high or moderate electrical conductivity $\sigma_{np}$ and low work function $\phi$. Thus, the electrons injected under the action of enhanced emission at the tip, are ready converted into negative ions by the already strong attachment to the host liquid at locations with electric fields lower than $E_s$. Even though the presence of the nanoparticles can scavenge electrons, this process is negligible compared with attachment even under ZnO–$C_{18}$ concentration of up to 1%wt (as inferred from figure 4). Consequently, the electrostatic shielding produced by the negative charge carriers (mainly negative ions) is unaffected by changes in the nanoparticle concentration as shown in figure 7.

Similarly, the simulation results also show that the decrease of the electron velocity predicted by the shallow trap hypothesis [11, 20] has no effect in the surface electric field $E_{tip}$. Even if the higher density of traps produced in the nanofluid would also increase the rate of attachment in the liquid as suggested in [11], such a process

would be proportional to the nanoparticle concentration. However, this suggestion is also not supported by the estimated $E_{tip}$ as the size of the negative ion cloud in front of the needle tip is independent of the nanoparticle concentration.

On the other hand, the streamer inception in hydrocarbons under negative polarity is generally evaluated using the Townsend-Meek criterion in gases [32]. This criterion relates the inception of the discharge to the critical size $N_{crit}$ of an avalanche started with $n_0$ electrons, estimated as [58]:

$$n_0 e^{\int_{z_{tip}}^{z_{E_s}} (\alpha_{imp}(z) - \eta_{att}(z))\, dx} = n_0 e^C = N_{crit} \tag{22}$$

where $C$ is a dimensionless parameter representing the effective ionization integral from the needle tip at $z_{tip}$ to the location $z_{E_s}$ where the electric field is equal to $E_s$. In other words, $C$ represents the net number of ionization events a single electron produces as an avalanche propagates. Typical values of $C$ between 5 and 10 have been estimated for hydrocarbons at their streamer inception voltages [32], by using the Laplacian electric field distribution and assuming $n_0 = 1$. Based on the EHD model results, the effective ionization integral $C$ can be directly estimated under the total electric field including the space charge contribution. The $C$ here estimated for mineral oil under the experimental conditions in [17] is equal to 5.4, while for the nanofluid it is 3.2. Observe that the lower $C$ in the nanofluid compared with that in the host liquid is caused by the different number of electrons $n_0$ initiating the avalanches in both cases.

In the literature, it has been stated that one possible mechanism of negative streamer inception is liquid boiling [53]. Although the energy continuity equation (as in [12]) could be readily added to the model in order to calculate temperature, its estimates already show that the pressure induced by electrostrictive forces [29] at the needle is in the order of several thousand atmospheres. Under such high pressures, there are significant changes in some thermodynamical properties of hydrocarbons [59] compared with atmospheric conditions, which are unknown for mineral oil. Therefore, any estimate of the joule heating produced by the conduction currents in mineral oil would be unreliable when only thermodynamic properties at room conditions are used. Moreover, there is no phase diagram information of the used mineral oil at such intense pressures as to enable a proper assessment of boiling in the liquid at the streamer inception. For these reasons, no further assessment of liquid boiling in mineral oil or in the ZnO–$C_{18}$ nanofluid has been here attempted.

## 5. Conclusions

In this work, high-field conduction currents measured under both polarities and a detailed electrohydrodynamic model are used to quantitatively characterize the electron generation and loss mechanisms in mineral oil as a host liquid for ZnO–$C_{18}$ nanofluids. Furthermore, conduction current measurements in ZnO–$C_{18}$ nanofluids under a sharp negative needle-plane electrode configuration are used to characterize additional high-field processes present when nanoparticles are dispersed in the host liquid. In this manner, the simulation model is tuned to estimate the drift and generation of charged carriers at high fields in mineral oil and ZnO–$C_{18}$ nanofluids, such that the predicted currents are in good agreement with the measurements. As in a recent study, the model results show that high field generation of electrons in mineral oil can be described by generalized equations usually attributed to Zener molecular ionization and electron impact ionization. Zener molecular ionization acts as the source of initial electrons in front of the negative needle surface at fields larger than about $1 \times 10^8$ V/m. As these initial electrons drift, they multiply due to the impact ionization. It is also found that electron attachment decreases with electric field. Electron attachment is a dominant process at fields lower than $3 \times 10^8$ V/m at which it overcomes the generation of electrons caused by impact ionization. Consequently, the avalanches penetrate into the liquid only a distance of few micrometres from the electrode tip since the electric field is highly divergent at close proximity to the needle.

The model results suggest that enhanced electron field emission takes place due to the ZnO–$C_{18}$ nanoparticle aggregates standing on the negative needle surface, in addition to the generation processes already taking place in the host liquid. This field cold emission is enhanced due to the intensified electric field at the surface of the nanoparticle and by the low work function of ZnO. As a consequence, there is a large injection of electrons into the liquid in the presence of nanoparticles, which causes the negative conduction currents measured at high electric fields in ZnO–$C_{18}$ nanofluids to be more than an order of magnitude larger than those in mineral oil. Additionally, it is found that even though ZnO–$C_{18}$ nanoparticles scavenge electrons, the frequency of this process is negligible compared with the loss of electrons due to attachment in the host liquid. For this reason, the negative conduction currents measured at high electric fields in ZnO–$C_{18}$ nanofluids are not influenced by the concentration of the dispersed nanoparticles.

The electrohydrodynamics processes in mineral oil and ZnO–$C_{18}$ nanofluids just before negative streamer inception have also been analysed. The results show that negative ions in the host liquid and its associated ZnO–$C_{18}$ nanofluid electrically shield the needle, reducing its surface electric field. In the case of the ZnO–$C_{18}$

nanofluid, this shielding is more significant than in mineral oil due to the intensified production of negative carriers under the enhanced electron emission. Thus, the total electric field at the needle tip when streamers are initiated in the nanofluid reach the same level of about $2.5 \times 10^9$ V/m as in the case of mineral oil, even if the streamer inception voltage in the presence of the nanoparticles is significantly larger than in the host liquid. However, the estimated net number of ionization events a single electron produces as an avalanche propagates when streamers are initiated is different between the ZnO–$C_{18}$ nanofluid and mineral oil due to their different number of initial seed electrons in both cases.

Last, it is shown that the scavenging hypothesis of nanofluids is not valid for ZnO–$C_{18}$ nanofluids under negative needles. This hypothesis mistakenly presumes that scavenging of electrons by the dissolved nanoparticles in the nanofluid dominate over the attachment processes in mineral oil. For this reason, it fails to explain the weak dependence of the measured conduction currents or the streamer inception on the nanoparticle concentration in the tested nanofluid. Similarly, it is shown that the reduction of the electron mobility by the nanoparticles in the shallow trap hypothesis has not effect on the simulated conduction currents or the needle electric field at the streamer inception voltage in ZnO–$C_{18}$ nanofluids. These results cast serious doubts on the general validity of those two theories of the breakdown improvement for other nanofluids in mineral oil. However, further studies are necessary to conclusively state whether these two theories are valid or not to explain the enhancement of the dielectric strength of mineral oil when using other nanoparticles.

## Acknowledgments

The technical support of Janne Nilsson during the development of the set-up used in the experiments is highly appreciated.

## Data availability statement

The data that support the findings of this study are available upon reasonable request from the authors.

## Funding

M.A. would like to thanks Colciencias for the funds received for this research. M.B. would like to acknowledge the financial support of the Swedish strategic research program StandUp for Energy.

## Conflicts of interest

The authors declare no conflict of interest.

## ORCID iDs

Marley Becerra https://orcid.org/0000-0002-6375-6142
Mauricio Aljure https://orcid.org/0000-0002-8173-8765
Amir Masoud Pourrahimi https://orcid.org/0000-0001-5867-0531

## References

[1] Ahmad F, Khan A A, Khan Q and Hussain M R 2019 State-of-art in nano-based dielectric oil: a review *IEEE Access* **7** 13396–410
[2] Fal J, Mahian O and Żyła G 2018 Nanofluids in the service of high voltage transformers: breakdown properties of transformer oils with nanoparticles, a review *Energies* **11** 2942
[3] Primo V A, Garcia B and Albarracin R 2018 Improvement of transformer liquid insulation using nanodielectric fluids: A review *IEEE Electr. Insul. Mag.* **34** 13–26
[4] Yi J 2016 Breakdown properties of mineral oil and ester based TiO2 and BN nanofluids *PhD thesis* University of Strathclyde
[5] Aljure M, Becerra M and Karlsson M E 2019 On the injection and generation of charge carriers in mineral oil under high electric fields *Journal of Physics Communications* **3** 15
[6] Lesaint O 2016 Prebreakdown phenomena in liquids: propagation 'modes' and basic physical properties *J. Phys. D: Appl. Phys.* **49** 144001
[7] Beroual A 2016 Pre-breakdown mechanisms in dielectric liquids and predicting models *2016 IEEE Electrical Insulation Conference (EIC)* **2016** 117–28
[8] Dumitrescu L, Lesaint O, Bonifaci N and Denat A 2001 and Notingher, Study of streamer inception in cyclohexane with a sensitive charge measurement technique under impulse voltage *J. Electrostat.* **53** 135–46

[9] Hestad O, Lundgaard L and Linhjell D 2010 New experimental system for the study of the effect of temperature and liquid to solid transition on streamers in dielectric liquids: application to cyclohexane *IEEE Trans. Dielectr. Electr. Insul.* **17** 764–74
[10] Jin H, Morshuis P, Mor A R, Smit J J and Andritsch T 2015 Partial discharge behavior of mineral oil based nanofluids *IEEE Trans. Dielectr. Electr. Insul.* **22** 2747–53
[11] Zhou Y, Sui S, Li J, Ouyang Z, Lv Y, Li C and Lu W 2018 The effects of shallow traps on the positive streamer electrodynamics in transformer oil based nanofluids *J. Phys. D: Appl. Phys.* **51** 105304
[12] O'Sullivan F 2007 A model for the initiation and propagation of electrical streamers in transformer oil and transformer oil based nanofluids *PhD thesis* Massachusetts Institute of Technology
[13] Jin H, Andritsch T, Morshuis P H F and Smit J J 2012 AC breakdown voltage and viscosity of mineral oil based SiO2 nanofluids *2012 Annual Report Conference on Electrical Insulation and Dielectric Phenomena* (Montreal, QC) **2012** 902–5
[14] Jin H, Morshuis P H, Mor A R and Andritsch T 2014 An investigation into the dynamics of partial discharge propagation in mineral oil based nanofluids *2014 IEEE 18th International Conference on Dielectric Liquids (ICDL)* **2014** 1–4
[15] Jin H, Andritsch T, Tsekmes I A, Kochetov R, Morshuis H F, Smit J J and Jin H 2014 Properties of mineral oil based silica nanofluids *IEEE Trans. Dielectr. Electr. Insul.* **21** 1100–8
[16] Jin H, Morshuis P H, Smit J J and Andritsch T 2014 The effect of surface treatment of silica nanoparticles on the breakdown strength of mineral oil *2014 IEEE 18th International Conference on Dielectric Liquids (ICDL)* **2014** 1–4
[17] Aljure M, Becerra M and Karlsson M 2018 Streamer inception from ultra-sharp needles in mineral oil based nanofluids *Energies* **11** 14
[18] Aljure M 2019 Pre-breakdown phenomena in mineral oil based nanofluids *PhD thesis* KTH Royal Institute of Technology
[19] Hwang J G, Zahn M, O'Sullivan F M, Pettersson L A A, Hjortstam O, Liu R, O'Sullivan F M, Pettersson L A A, Hjortstam O and Liu R 2010 Effects of nanoparticle charging on streamer development in transformer oil-based nanofluids *J. Appl. Phys.* **107** 014310
[20] Wang Z, Zhou Y, Lu W, Peng N and Chen W 2019 The impact of TiO2 nanoparticle concentration levels on impulse breakdown performance of mineral oil-based nanofluids *Nanomaterials* **9** 627
[21] Du Y, Lv Y, Li C, Chen M, Zhou J, Li X, Zhou Y and Tu Y 2011 Effect of electron shallow trap on breakdown performance of transformer oil-based nanofluids *J. Appl. Phys.* **110** 104104
[22] Tanaka T, Kozako M, Fuse N and Ohki Y 2005 Proposal of a multi-core model for polymer nanocomposite dielectrics *IEEE Trans. Dielectr. Electr. Insul.* **12** 669–81
[23] Negri F and Cavallini A 2015 Analysis of conduction currents in nanofluids *2015 IEEE Conference on Electrical Insulation and Dielectric Phenomena (CEIDP)* **2015** 27–30
[24] Li Y, Dong M, Zhang C, Xie J, Ren M, Zhou J and Dai J 2018 Investigation on charge-carrier transport characteristics of transformer oil-based nanofluids *IEEE Trans. Dielectr. Electr. Insul.* **25** 2443–51
[25] Becerra M, Frid H and Vázquez P A 2017 Self-consistent modeling of laminar electrohydrodynamic plumes from ultra-sharp needles in cyclohexane *Phys. Fluids* **29** 123605
[26] Aljure M, Becerra M and Pallon L K H 2016 Electrical conduction currents of a mineral oil-based nanofluid in needle-plane configuration *2016 IEEE Conference on Electrical Insulation and Dielectric Phenomena (CEIDP)* **2016** 687–90
[27] Nynas A B 2017 Nytro 10X safety data sheet p 1–36
[28] Pourrahimi A M, Hoang T A, Liu D, Pallon L K H, Gubanski S, Olsson R T, Gedde U W and Hedenqvist M S 2016 Highly efficient interfaces in nanocomposites based on polyethylene and ZnO nano/hierarchical particles: a novel approach toward ultralow electrical conductivity insulations *Adv. Mater.* **28** 8651–7
[29] Lahoz D 1980 Force density in fluid dielectrics *Phys. Lett.* A **79** 181–2
[30] COMSOL, Comsol Multiphysics v. 5.4
[31] Morrow R and Sato N 1999 The discharge current induced by the motion of charged particles in time-dependent electric fields; Sato's equation extended *J. Phys. D: Appl. Phys.* **32** L20–2
[32] Naidis G V 2015 Modelling of streamer propagation in hydrocarbon liquids in point-plane gaps *J. Phys. D: Appl. Phys.* **48** 195203
[33] Jadidian J 2013 Charge transport and breakdown physics in liquid/solid insulation systems *PhD thesis* Massachusetts Institute of Technology
[34] Zadeh M S 2011 Measurement of ion mobility in dielectric liquids *Master thesis* Chalmers University of Technology
[35] Zener C 1934 A theory of the electrical breakdown of solid dielectrics *Proceedings of the Royal Society A: Mathematical, Physical and Engineering Sciences* **145** 523–9
[36] Devins J C, Rzad S J and Schwabe R J 1981 Breakdown and prebreakdown phenomena in liquids *J. Appl. Phys.* **52** 4531–45
[37] O'Sullivan F, Hwang J G J, Zahn M, Hjortstam O, Pettersson L, Biller P, Liu R and Biller P 2008 A model for the initiation and propagation of positive streamers in transformer oil *Conference Record of the 2008 IEEE International Symposium on Electrical Insulation* **2008** 210–4
[38] Naidis G V 2015 On streamer inception in hydrocarbon liquids in point-plane gaps *IEEE Trans. Dielectr. Electr. Insul.* **22** 2428–32
[39] Haidara M and Denat A 1991 Electron multiplication in liquid cyclohexane and propane *IEEE Trans. Electr. Insul.* **26** 592–7
[40] Derenzo S E, Mast T S, Zaklad H and Muller R A 1974 Electron avalanche in liquid xenon *Phys. Rev.* A **9** 2582–91
[41] Holroyd R 1988 Electron kinetics in nonpolar liquids — energy and pressure effects *The Liquid State and Its Electrical Properties* (Plenum Press) 221–33
[42] Hwang J G, Zahn M and Pettersson L A A 2012 Mechanisms behind positive streamers and their distinct propagation modes in transformer oil *IEEE Trans. Dielectr. Electr. Insul.* **19** 162–74
[43] Optimization Module User's Guide. Stockholm, Sweden: Comsol Multiphysics, 2018
[44] Zhang Z, Meng G, Wu Q, Hu Z, Chen J, Xu Q and Zhou F 2015 Enhanced cold field emission of large-area arrays of vertically aligned ZnO-nanotapers via sharpening: experiment and theory *Sci. Rep.* **4** 4676
[45] Forbes R G and Deane J H 2007 Reformulation of the standard theory of fowler–nordheim tunnelling and cold field electron emission *Proceedings of the Royal Society A: Mathematical, Physical and Engineering Sciences* **463** 2907–27
[46] Schmidt W F and Illenberger E 2003 Low energy electrons in non-polar liquids *International Journal of Nuclear Research* **48** 75–82
[47] Gutmann S, Conrad M, Wolak M A, Beerbom M M and Schlaf R 2012 Work function measurements on nano-crystalline zinc oxide surfaces *J. Appl. Phys.* **111** 123710
[48] Denat A, Gosse J and Gosse B 1988 Electrical conduction of purified cyclohexane in a divergent electric field *IEEE Trans. Electr. Insul.* **23** 545–54
[49] Lv Y, Du Q, Wang L, Sun Q, Huang M, Li C and Qi B 2017 Effect of TiO 2 nanoparticles on the ion mobilities in transformer oil-based nanofluid *AIP Adv.* **7** 105022
[50] Chen G, Given M, Timoshkin I, Wilson M P and MacGregor S 2017 Measurements of mobility in aged mineral oil in the presence of nanoparticles *2017 IEEE 19th International Conference on Dielectric Liquids (ICDL)* **2017** 1–4

[51] Halpern B and Gomer R 1969 Field emission in liquids *J. Chem. Phys.* **51** 1031–47
[52] Lundgaard L, Linhjell D, Hestad ØL, Unge M and Hjortstam O 2020 Pre-breakdown phenomena in hydrocarbon liquids in a point-plane gap under step voltage. Part 2: behaviour under negative polarity and comparison with positive polarity *Journal of Physics Communications* **4** 045011
[53] Denat A 2006 High field conduction and prebreakdown phenomena in dielectric liquids *IEEE Trans. Dielectr. Electr. Insul.* **13** 518–25
[54] Velasco J, Frascella R, Albarracín R, Burgos J, Dong M, Ren M and Yang L 2018 Comparison of positive streamers in liquid dielectrics with and without nanoparticles simulated with finite-element software *Energies* **11** 361
[55] Jadidian J, Zahn M, Lavesson N, Widlund O and Borg K 2013 Stochastic and deterministic causes of streamer branching in liquid dielectrics *J. Appl. Phys.* **114** 063301
[56] Jadidian J, Zahn M, Lavesson N, Widlund O and Borg K 2012 Effects of impulse voltage oolarity, peak amplitude, and rise time on streamers initiated from a needle electrode in transformer oil *IEEE Trans. Plasma Sci.* **40** 909–18
[57] Denat A 2011 Conduction and breakdown initiation in dielectric liquids *2011 IEEE International Conference on Dielectric Liquids* (Trondheim, Norway) **2011** 1–11
[58] Meek J and Craggs J 1978 *Electrical breakdown of gases* (New York: John Wiley & Sons)
[59] Kashiwagi H and Makita T 1982 Viscosity of twelve hydrocarbon liquids in the temperature range 298-348 K at pressures up to 110 MPa *Int. J. Thermophys.* **3** 289–305